P-48

Annual Progress Report

Submitted to:

National Aeronautics and Space
Administration, Langley Research Center
Hampton, Va 23665-5225
Atten: Mr. Michael D. Williams
Technical Officer, M/S 493.

Institution:

Hampton University
Dept. of Physics
Hampton, Va 23668

Title of Research:

Plasma Puff Initiation of
High Coulomb Transfer Switches

NASA Grant No: NAG-1-970

Period Covered: Oct. 1, 1989 -- Sept 30, 1990

Principal Investigator: D. D. Venable

Research Assistant Professor: E. H. Choi

N91-10735

(NASA-CR-187024) PLASMA PUFF INITIATION OF HIGH COULOMB TRANSFER SWITCHES Annual Progress Report, 1 Oct. 1989 - 30 Sep. 1990 (Hampton Inst.) 48 p CSCL 20I

Unclas G3/75 0309069

Table of Contents

Plasma-Puff Initiation of High Coulomb Transfer Switches

Abstract

The plasma-puff triggering mechanism based on a hypocycloidal pinch geometery was investigated to determine the optimal operating conditions for the azimuthally uniform surface flashover which initiates plasma-puff under wide ranges of fill gas pressure of Ar, He and N_2. The optimal fill gas pressure for the azimuthally uniform plasma-puff was about 120 mTorr $< P_{opt} <$ 450 Torr for He and N_2. For Argon 120 mTorr $< P_{opt} <$ 5 Torr. The inverse pinch switch was triggered with the plasma-puff and the switching capability under various electrical parameters and working gas pressures of Ar, He and N_2 was determined. It was also shown that the azimuthally uniform switching discharges were dependent on the type of fill gas and its fill pressure. A new concept of plasma-focus driven plasma-puff was also discussed in comparison with the hypocycloidal pinch plasma-puff triggering. The main discharge of

inverse pinch switch with plasma-focus driven plasma-puff trigger is found to be more azimuthally uniform than that with hypocycloidal pinch plasma-puff trigger in a gas pressure region between 80 mTorr and 1 Torr.

I. Introduction

This report covers the period from February, 1989 to February 1990 of NASA Grant NAG1-970 entitled "Plasma-Puff Initiation of High Coulomb Transfer Switches".

New developments in high pulse power systems, such as lasers[1], intense relativistic electron beam accelerators[2], and fusion devices[3], often require electrical switching capabilities beyond what are currently available. The requirements for a high power switch are, in general, fast rise time, high current handling capability, fast recovery time (which affects the repetition rate), fast thermal energy dissipation, free from component damage, and high hold-off voltage. In addition, reproducibility of switching action and a long lifetime are particularly emphasized for space application of magnetoplasmadynamic (MPD) thruster technology[4].

Spark gap swiches, commonly used for high pulse-power commutation, have short lifetimes because of severe electrode heating from which surface erosion occurs even though this switch still covers the highest transfer range[5]. Also the important requirement of a fast recovery time has not been successfully realized in the spark gap.

One approach which has been taken to provide a high coulomb tranfer switch having a longer useful life, higher current capability and faster switching than those of existing high power switches has been developed by Lee[6] (U.S. Pat. No. 4475066). The inverse pinch structure is designed to carry high currents with significantly reduced erosion of electrodes and to reduce the inductance of the switch by using coaxial current paths. Preliminary results show that the peak current handling capability was larger than 350 kA at a hold-off voltage of 14 kV when N_2 fill gas pressure was 10 mTorr[7]. An upgrading design for an inverse pinch switch is recently reported to meet the requirements for the output switch of an ultra-high-power (>30 GW) pulser[8]. The hold-off voltage of 1 MV is met by adopting multistage rim-fire electrodes and using SF_6 as the dielectric gas of the switch[8].

For the inverse pinch switch, an initial uniform breakdown is a key factor for obtaining reproducibility and for long-life operation. Accordingly, the development of an inverse pinch current in the switch depends on the trigger mechanism. In the preliminary experiment, the triggering of the switch was provided by a pin type[9] or ring type third electrode[9], and azimuthally uniform initiation was limited to a narrow range of working gas pressures. By using the trigger pins with a trigger pulse having 100 ns rising time, a switching phase reproduction of less than 20% at a pressure of 10 mTorr was observed. This indicates that a fast trigger pulse is required to increase the reproducibility. The wear of the trigger pins is eminent and the switch therfore has a short lifetime.

In this research, a new triggering mechanism called "plasma-puff", was designed and investigated to determine the operating conditions for a wide range of filling gas pressures of Ar, He and N_2. A prototype of the plasma inverse pinch switch with plasma-puff trigger was tested[10] to characterize the hold-off voltage, the anode-fall time, the switch resistance, the energy dissipation, the recovery time, and the V-I phase relation with a high current load of 0.5 MA. The plasma-puff trigger electrode are coaxially located under the main gap electrode pair and initiates gap breakdown by injecting annular plasma rings into the gap. The major advantages of the plasma-puff trigger is a circumferentially uniform current sheet formed by the initial surface discharge which in turn could initiate an uniform annular breakdown over the insulator in the main gap of the inverse pinch switch. The plasma-puff triggering device is in a hypocycloidal pinch[11] geometry and drives the current sheet (plasma) radially inward into the annular gap of the main electrode. The plasma driven by the current sheet, i.e., the plasma-puff, produces electrons and ions for the main gap breakdown.

An another new triggering concept of plasma-focus driven plasma-puff was designed and tested to determine the operating conditions and optimization of this method for the azimuthally uniform switching discharges for a wide range of fill gas pressures of Ar, He and N_2. The trigger electrode in this geometry are coaxially located above the main gap electrode pair and insulated by teflon from the main gap electrode. The plasma-puff triggering device is in a plasma-focus geometry and drives the current sheet axially downward and radially inward into the annular gap of the main electrode. The plasma-focus driven plasma produces electrons and ions for the main switch breakdown.

This report was devoted to installation and operation of the above two kinds of new trigger devices for a wide pressure ranges of Ar, He and N_2.

II. Experimental Configuration and Diagnostics

II A. Hypocycloidal Pinch Plasma-Puff Trigger

The experimental apparatus consists of a plasma-puff device based on the hypocycloidal pinch[11] geometry, a high voltage power supply, a six stage Marx generator, a trigger initiator using a thyratron, a capacitor bank, and a vacuum/gas handling unit. The systems of the inverse pinch switch and the capacitor bank with a high voltage power supply are installed when the switching capability experiment is performed. The trigger and charging voltages in the Marx generator are provided by a trigger initiator with a thyratron and a high voltage power supply, respectively.

The trigger pulse from the Marx generator has a rise-time of 10 ns and jitter less than 10 ns. The four parralel electrical outputs from the Marx generator are split into eight parallel electrical outputs, using 50 ohm loads. The Marx generator has a net capacitance of C_M = 1.67 nF when erected to produce an output voltage of 6 times that of the charging voltage. The capacitor bank id composed of 3 capacitors in parallel having a total storage energy of 1.6 kJ, a total capacitance of 8.1 uF, and a voltage of up to 20 kV.

Figure 1 shows a scematic diagram of the plasma-puff triggering experiment. Figure 2a shows s cut away view of the plasma-puff triggering device. Dual beam oscilloscopes and an image converter camera (ICC) were used as diagnostic tools. The ICC camera was set in the focus mode to take a picture of the area of emission from the puffed plasma and the angular distribution of the plasma emission was studied. The electrical parameters of the circuit are obtained from Rogowski coils and voltage dividers. The Rogowski coil is coupled with an RC = 160 us integrating circuit to obtain the switching current from its output voltage. The switching current is linearly proportional to the output signal of the Rogowski coil with the RC integrating circuit.

The hypocycloidal pinch plasma-puff triggering device, which is coaxially located below the outer electrode of the inverse pinch switch has a diameter of 6.0 cm. The gap distance between the trigger and ground electrodes is 2.45 cm. When trigger pulse is applied in this geometry, there is a surface breakdown over the insulator which initiates plasma-puff.

To determine the operating range for obtaining azimuthally uniform plasma-puff, tests were performed for a wide range of gas pressures of Ar, He and N_2. In this experiment, the charging voltages for the Marx generator have been set at 10, 15, and 20 kV which results in trigger voltages of 60, 90, and 120 kV, respectively. For the given charging voltage, the gas pressures have been varied from 40 mTorr to 600 Torr.

The plasma-puff device was finally combined with the inverse pinch plasma switch to test the switching capability as shown in Fig. 2b. The diagnostics equipment for the switch operation was composed of the high voltage probe for the measurement of voltage, the Rogowski coil for the measurement of time dependent current shape and the image converter camera in the framing mode for the observation of switch action.

II B. Plasma-Focus Driven Plasma-Puff Trigger

The experimental apparatus consists of a plasma-puff device based on the plasma-focus Mather geometry[12], a high voltage power supply, a trigger initiator using a thyratron, a capacitor bank, and a vacuum/gas handling unit. The Marx generator is not used in this experiment.

The trigger pulse from the trigger initiator is connected to the top of an outer trigger electrode which is insulated from inner electrode by teflon. Figure 3 shows a schematic diagram of the plasma-focus driven plasma-puff triggering experiment. The diagnostic techniques are same as those of hypocycloidal pinch plasma-puff trigger.

The gap distance between the trigger (outer) electrode and ground (inner) electrode is 4.1 mm. The path of surface flashover along the insulator surface of teflon which is attached onto the inner electrode is 1.63 cm. With this geometry, there is a surface breakdown which initiates plasma-focus driven plasma-puff.

Tests were performed to determine the operating range of azimuthally uniform breakdown in plasma-focus driven plasma-puff triggering experiment for a wide range of gas pressures of Ar, He and N_2. In this experiment, the triggering voltage is kept at 12 kV and the gas pressures have been varied from 40 mTorr to 600 Torr.

III. Experimental Results and Discussion

III A. Hypocycloidal Pinch Plasma-Puff Trigger

Figure 4 shows the set up for the ICC photograph of the hypocycloidal pinch plasma-puff experiment, and Fig. 5 shows the ICC focus mode pictures of the surface breakdown initiated plasma-puff at several N_2 gas pressures under a charging voltage of 15 kV to the Marx generator. It was found that the ranges of gas pressure where the angle (θ_{disc}) of plasma emission is 360^o are broaden as the charging voltage is increased to 20 kV. In Fig. 6a, the angle of plasma emission is plotted asa function of the nitogen gas pressure for several charging voltages to the Marx generator. θ_{disc} is represented by the symbols of solid square, circle, and triangle corresponding to the charging voltages of 10 kV, 15 kV and 20 kV, respectively. Under the charging voltage of 10 kV (3.0 J) the azimuthally uniform surface breakdown of plasma-puff occurs from 250 mTorr to approximately 150 Torr of fill gas pressures. With a 15 kV (6.75 J) charging voltage, the azimuthally uniform surface breakdown occurs from 200 mTorr up to approximately 400 Torr of

N_2 gas pressure. In the case of 20 kV (12.02 J) charging voltage, similar results were obtained for the pressure range of 150 mTorr to 475 Torr. In Fig. 6b, the angle of plasma emission is plotted as a function of gas pressure for gases of Ar, He and N_2 under the charging voltage of 15 kV to the Marx generator. The symbols used in Fig. 6b are triangle, square and cross corresponding to N_2, He and Ar, respectively. It is also observed from the information given in Figs. 6a and 6b that the optimal operating gas pressure (P_{opt}) range for azimuthally uniform plasma-puff is about 120 mTorr < P_{opt} <450 Torr for He and N_2. For argon the the optimal pressure range is shown to be a narrow range of 120 mTorr < P_{opt} < 5 Torr, and beyond that the trigger discharging angle is only about 180^o as shown in Fig. 6b.

Figure 7 shows the number of hot spots produced in the hypocycloidal pinch plasma-puff discharge as a function of N_2 gas pressure for various charging voltages. The symbols used here are identical with those of Fig. 6a. It is shown that the hot spots are not generated up to 4 Torr gas pressure. However, there is no more than one hot spot in the optimal region of gas pressure for all three charging voltages and gases of Ar, He and N_2.

In Fig. 8, the current and voltage waveforms for hypocycloidal pinch plasma-puff trigger are represented in the upper and lower images, respectively. These data were obtained for a pressure of 45 Torr and a charging voltage of 10 kV to the Marx generator. The peak current and voltage are found to be 32 kA and 58 kV, respectively. Both signals have a period of 150 ns, which corresponds to the ringing frequency of 6.6 MHz. The current risetime and dI/dt are found to be 50 ns and 6×10^{11} A/s, respectively, from Fig. 8. The inductance and resistance of the hypocycloidal pinch plasma-puff triggering system are found to be 0.6 uH and 2 ohm, respectively.

The plasma-puff device was combined with the inverse pinch plasma switch to test the switching capability. The schematic diagram of the diagnostics equipment is shown in Fig. 9. In Fig. 10, the hold-off voltages of the inverse pinch switch are represented as a function of pressure for gases of Ar, He and N_2. The hold-off voltage is represented by the symbols of cross, square and triangle corresponding to the Ar, He and N_2, respectively. It is shown that the pressure of minimum hold-off voltages are 200 mTorr, 2 Torr and 10

Torr for N_2, Ar and He, respectively. In general the hold-off voltages of the inverse pinch plasma switch for Ar and N_2 as a function of pressure exibit the behavior of the Paschen's curve as expected. For helium, the holf-off voltages of the inverse pinch switch below 300 mTorr are not similar to those of parallel plates because of impurities coming from leakage. At the lower gas pressures between 50 mTorr and 200 mTorr, the holf-off voltages of the inverse pinch switch are shown to be similar values and less than 500 V for gases of Ar, N_2 and He. However, the hold-off voltages are increased as the gas pressures are increased as expected. The hold-off voltages of inverse pinch switch for He, Ar and N_2 are observed to be about 1.2 kV, 2 kV and 10 kV, respectively, at gas pressure of 200 Torr.

In Fig. 11, the voltage and current waveforms of inverse pinch plasma switch are represented in the upper and lower pictures, respectively. these data were obtained for a N_2 gas of 300 Torr under charging voltage of 13.5 KV to inner electrode of the inverse pinch switch. The peak current and voltage are found to be 80 kA and 12 kV, respectively. The measured peak current 80 kA is in good agreement with that of calculated value of 83 kA from elementary circuit theory. Both signals have a period of about 8 us, which corresponds to a ringing frequency of 125 kHz. The current risetime and dI/dt of inverse pinch switch are found to be 2 us and 4×10^{10} A/s, respectively. The inductance and resistance of the inverse pinch switch are found to be 195.5 nH and 10 mΩ, respectively. The measured and calculated current waveforms are plotted in Fig. 12 as a function of time, in which the symbols of solid square and square are corresponding to the measured and calculated values, respectively. Figure 12 shows that the both values are in good agreement with each other.

Figure 13 shows the frame mode photograph of the breakdown of the inverse pinch switch taken by the image converter camera with the first and second delay time to be 1.2 us and 0.5 us from first delay, respectively. In Fig. 13, the main charging voltage is kept at 9 kV and N_2 gas pressure is maintained at 150 Torr. The switch discharging angle with respect to the center of the inner electrode is shown to be about 180^o in this experimental condition. In Fig. 14, the main discharging angles of inverse pinch switch are plotted as a function of pressure for gases of Ar, He and N_2. They are represented by symbols of triangle, square and dot corresponding to the N_2, He and Ar, respectively. For argon gas, the azimuthally uniform switching action is occured at pressure region between 600 mTorr and 5 Torr, in which the triggering discharge is also azimuthally uniform. For N_2 and He, the main discharging angles are located between 90^o and 270^o for a wide ranges of gas pressure even though the triggering discharges are shown to be azimuthally uniform under the hypocycloidal pinch plasma-puff.

III B. Plasma-Focus Driven Plasma-Puff Trigger

The schematic diagram of the plasma-focus driven plasma-puff triggering experiment is shown in Fig. 3. The set up for the ICC photographing and the diagnostics for this experiment is basically same as those in section III A of hypocycloidal pinch plasma-puff trigger.

The optimal operating gas pressure (P_{opt}) range for N_2 gas is shown to be about 80 mTorr $< P_{opt} <$ 400 Torr for azimuthally uniform plasma-focus driven plasma-puff. This result is very similar to that for hypocycloidal pinch plasma-puff. For other gases of Ar and He, they are also similar to those of hypocycloidal pinch plasma-puff trigger.

In Fig. 15, the triggering voltage waveform for plasma-focus driven plasma-puff is represented under a pressure 40 mTorr and a charging voltage of 12 kV. The peak voltage is found to be 11 kV and its pulse width to be about 1.3 us. The peak current corresponding to its voltage signal is about 85 A. The triggering voltage risetime and dV/dt are found to be 0.6 us and 1.83×10^{10} V/s, respectively.

The voltage and current waveforms of inverse pinch plasma switch with plasma-focus driven plasma-puff trigger also similar to those with hypocycloidal pinch plasma-puff trigger. Also the inductance and resistance of the inverse pinch switch with plasma-focus driven plasma-puff trigger are similar to those with the hypocycloidal pinch plasma-puff trigger.

In Fig. 16, the main discharging angles of inverse pinch switch with plasma-focus driven plasma-puff trigger are plotted as a function of N_2 gas pressures. Solid triangles and triangles in Fig. 16 correspond to the plasma-focus driven and hypocycloidal pinch plasma-puff trigger, respectively. Figure 16 shows that the main discharge of inverse pinch switch with this plasma-puff trigger is more azimuthally uniform than that with hypocycloidal pinch plasma -puff trigger in a gas pressure region between 80 mTorr and 1 Torr. At relatively high pressure regime, the main discharging angles of inverse pinch switch with plasma-focus driven plasma-puff trigger are shown to be very similar to those with hypocycloidal pinch plasma-puff trigger. For other gases of Ar and He, the similar results are observed.

Figure 17 shows that the focussing mode photograph of the azimuthally uniform breakdown of the inverse pinch switch taken by the image converter camera. The N_2 gas pressure is kept at 160 mTorr and the triggering voltage ia maintained at 12 kV in this situation. Figure 18 shows the frame mode picture of the azimuthally uniform breakdown of the inverse pinch switch with plasma-focus driven plasma-puff trigger taken by the image converter camera with first delay and second delay time of 1.2 us and 0.5 us from first delay, respectively, at gas pressure of 800 mTorr. It is shown that the left hand lower side of switch breakdown becomes to be more intense as time is evolved from 1.2 us to 1.7 us as shown in Fig. 18. The main switching and triggering votages are kept at 0.6 kV and 12 kV, respectively, in this picture.

IV. Summary

The plasma-puff triggering mechanism based on a hypocycloidal pinch geometry and plasma-focus Mather geometry were investigated to determine the optimal operating conditions for the azimuthally uniform surface flashover which initiates plasma-puff under wide ranges of fill gas pressure if Ar, He and N_2. The optimal fill gas pressure for the azimuthally uniform plasma-puff was about 120 mTorr < P_{opt} < 450 Torr for He and N_2. For argon 120 mTorr < P_{opt} < 5 Torr. The inverse pinch switch was triggered with the plasma-puff and the switching capability under various electrical parameters and working gas pressures of Ar, He and N_2 was determined. It was also shown that the azimuthally uniform switching discharges were dependent on the type of fill gas and its fill pressure. The main discharge of inverse pinch switch with plasma-focus driven plasma-puff trigger is proved to be more azimuthally uniform than that with hypocycloidal pinch plasma-puff

trigger in a gas pressure region between 80 mTorr and 1 Torr.

A hold-off voltage greater than the test voltage used here will be requierd for the inverse pinch switch for future applications. It might be necessary to adopt a multi-ring and multi-gap arrangement to obtain the optimal switching operating conditions for such high voltage applications.

References

1) S. Watanabe, A. J. Alook, K. E. Leopold and R. S. Taylor, Appl. Phys. Lett. 38, 3 (1981).

2) B. Kulke, T. Immes, R. Kihara and R. Scarpetti, IEEE Conference Record of 1982 15th Power Modulator Symposium, p. 307 (1982).

3) R. G. Adams, D. R. Humphreys, J. R. Woodworth, M. M. Dillon, D. Green, and J. F. Seamen, IEEE Conference Record of 1984 16th Power Modulator Symposium p. 191 (1984).

4) J. S. Sovey and M. A. Mantenides, AIAA/ASME/SAE/ASEE 24th Joint Propulsion Conference, 1988.

5) A. E. Bishop and G. D. Edmonds, Proc. 5th Sym. Fusion Technology, Oxford, U. K. 1968.

6) J. H. Lee, U. S. Patent # 4475066, 1984.

7) S. H. Choi and J. H. Lee, Proc. of the 10th IEEE International Symposium on Discharges and Electrical Insulation in Vacuum, p 273 (1982).

8) J. H. Lee, S. H. Choi and K. D. Song, Proc. of the 7th IEEE Pulsed Power Conference, June(1989).

9) G. L. Schuster, J. H. Lee and S. H. Choi, Proc. of the 5th IEEE Pulsed Power Conference, p. 66 (1985).

10) M. T. Ngo, K. H. Schoenbach and J. H. Lee, APS Plasma Physics Division Meeting, L. A., November (1989).

11) J. H. Lee, D. R. Mcfarland, and F. Hohl, Phys. Fluids 20, 31 (1977).

12) J. W. Mather, Phys. Fluids 8, 366 (1965).

Figure Captions

Figure 1. Schematic diagram of the plasma-puff triggering experiment based on the hypocycloidal pinch geometry.

Figure 2a. Cut away view of the plasma-puff triggering device based on the hypocycloidal pinch geometry.

Figure 2b. Inversepinch combined with the hypocycloidal-pinch plasma-puff device.

Figure 3. Schematic diagram of the plasma-focus driven plasma-puff triggering experiment.

Figure 4. Schematic diagram for the spectroscopic and plasma dynamic measurements of the hypocycloidal pinch plasma-puff produced plasma.

Figure 5. ICC Focussing mode picture for the surface breakdown of hypocycloidal pinch plasma-puff at several N_2 gas pressures for a charging voltage of 15 kV to the Marx generator.

Figure 6a. Discharge angle (θ_{disc}) versus nitogen gas pressure for hypocycloidal pinch plasma-puff trigger. Solid squares, circles and triangles correspond to the charging voltages of 10 kV, 15 kV and 20 kV, respectively, to the Marx generator.

Figure 6b. Angle of plasma emission versus gas pressure of Ar, He and N_2 for hypocycloidal pinch plasma-puff trigger under the charging voltage of 15 kV to the Marx generator. Triangles, squares and crosses correspond to N_2, He and Ar, respectively.

Figure 7. Number of hot spots versus nitrogen gas pressure for hypocycloidal pinch plasma-puff trigger. The symbols used here are identical with those of Fig. 6a.

Figure 8. Triggering current (upper) and voltage (lower) waveform versus time for hypocycloidal pinch plasma-puff. These data were obtained with a gas pressure of 4 Torr and a charging voltage of 10 kV to the Marx generator.

Figure 9. Schematic diagram of the diagnostic equipment of the inverse pinch switch with the hypocycloidal pinch plasma-puff trigger.

Figure 10. Hold-off voltages of the inverse pinch switch versus

gas pressures of Ar, He and N_2. Crosses, squares and triangles correspond to the gases of Ar, He and N_2, respectively.

Figure 11. Voltage (upper) and current (lower) waveforms of inversepinch switch versus time. These data were obtained for a N_2 gas of 300 Torr under charging voltage of 13.5 kV to inner electrode of inverse pinch switch.

Figure 12. Measured and calculated current waveforms of the inverse pinch switch versus time. Solid squares and squares correspond to the measured and calculated values, respectively. These data were obtained under charging voltage of 13.5 kV to inner electrode of inverse pinch switch.

Figure 13. Frame mode photograph of the breakdown of the inverse pinch switch with the hypocycloidal pinch plasma-puff trigger taken by the image converter camera with the first and second delay times of 1.2 us and 0.5 us, respectively. The main charging voltage is kept at 9 kV and the N_2 gas pressure is maintained at 150 Torr.

Figure 14. Main discharging angles of inverse pinch switch with hypocycloidal pinch plasma-puff trigger versus pressure for gases of Ar, He and N_2. Triangles, squares and dots correspond to the N_2, He and Ar, respectively.

Figure 15. Triggering voltage waveform of plasma-focus driven plasma-puff versus time. This can be obtained under a N_2 gas pressure of 40 mTorr.

Figure 16. Main discharging angles of inverse pinch switch versus N_2 gas pressures with plasma-focus driven plasma-puff trigger and hypocycloidal pinch plasma-puff trigger.

Solid triangles and triangles correspond to the plasma-focus driven plasma-puff trigger and hypocycloidal pinch plasma-puff trigger, respectively.

Figure 17. Focussing mode photograph of the azimuthally uniform breakdown of the inverse pinch switch with the plasma-focus driven plasma-puff trigger taken by the image converter camera. The first and second delay times are set to be 1.2 us and 0.5 us, respectively. The N_2 gas

Figure 18. Frame mode photograph of the uniform breakdown of the inverse-pinch switch with the plasma-focus driven plasma-puff trigger taken by the image converter camara with the first and second delay times of 1.2 μs and .5 μs, respectively at gas pressure of 800 mTorr.

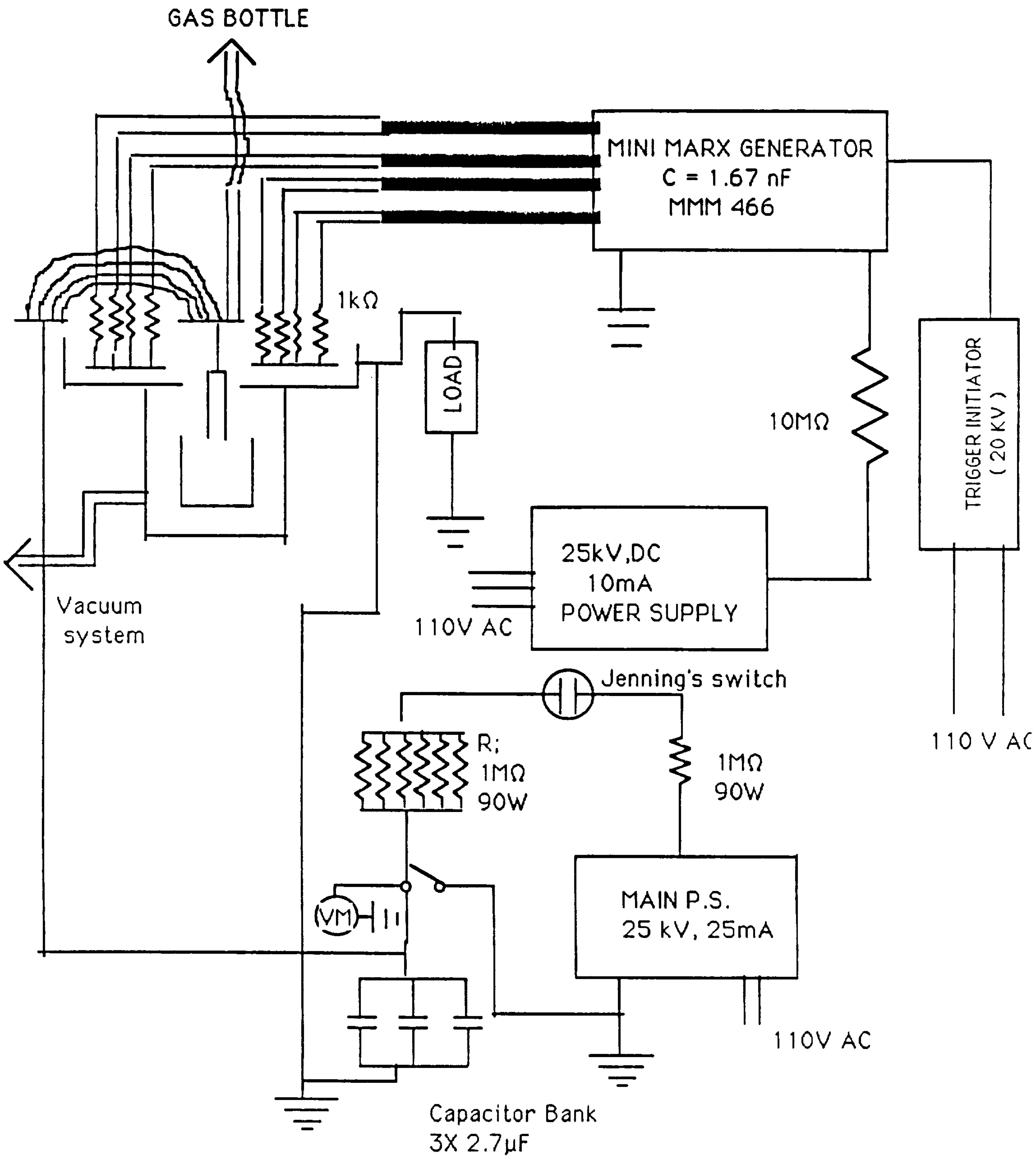

Figure 1. Schematic diagram of the plasma-puff triggering experiment based on the hypocycloidal pinch geometry.

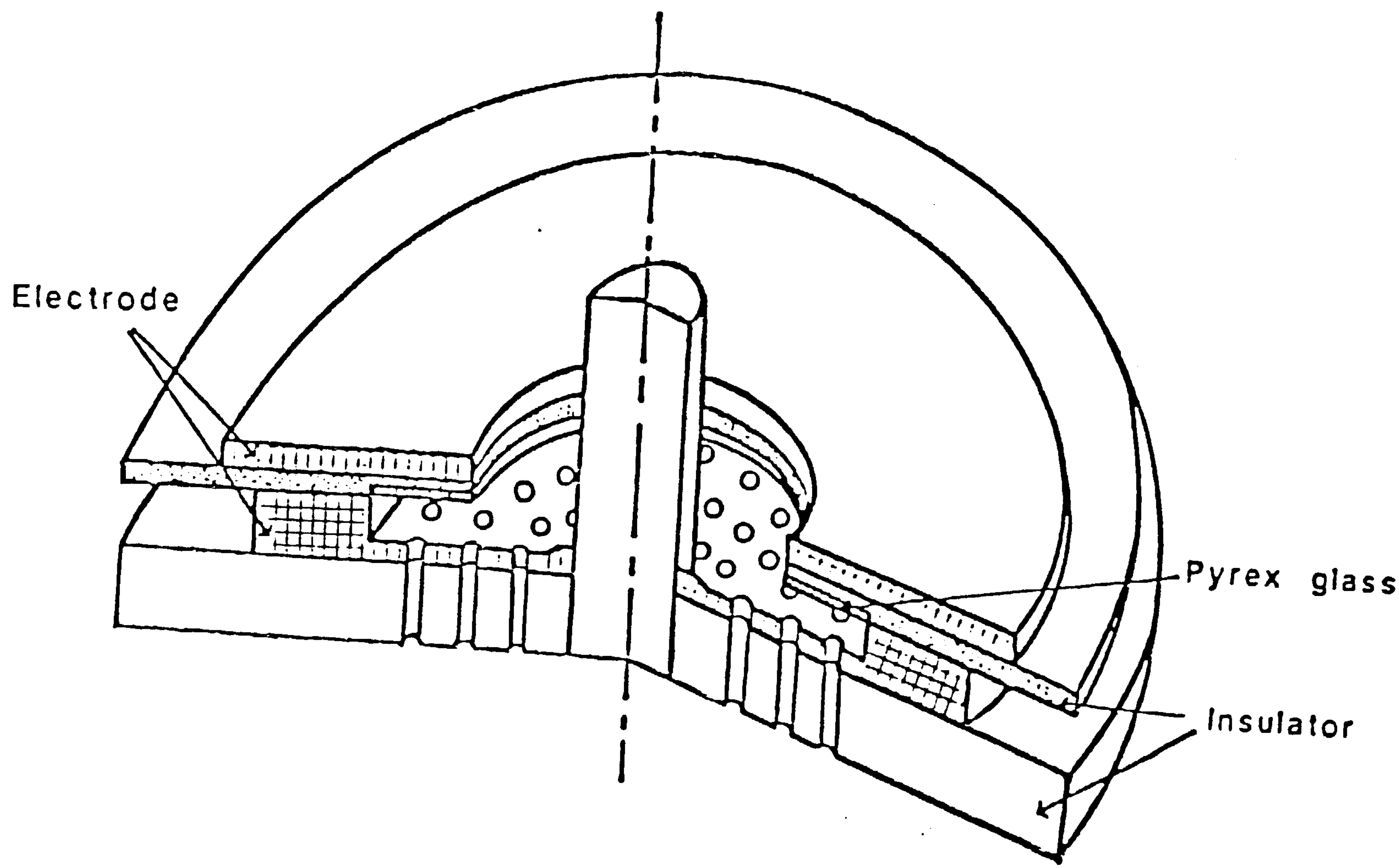

Figure 2a. Cut away view of the plasma-puff triggering device based on the hypocycloidal pinch geometry.

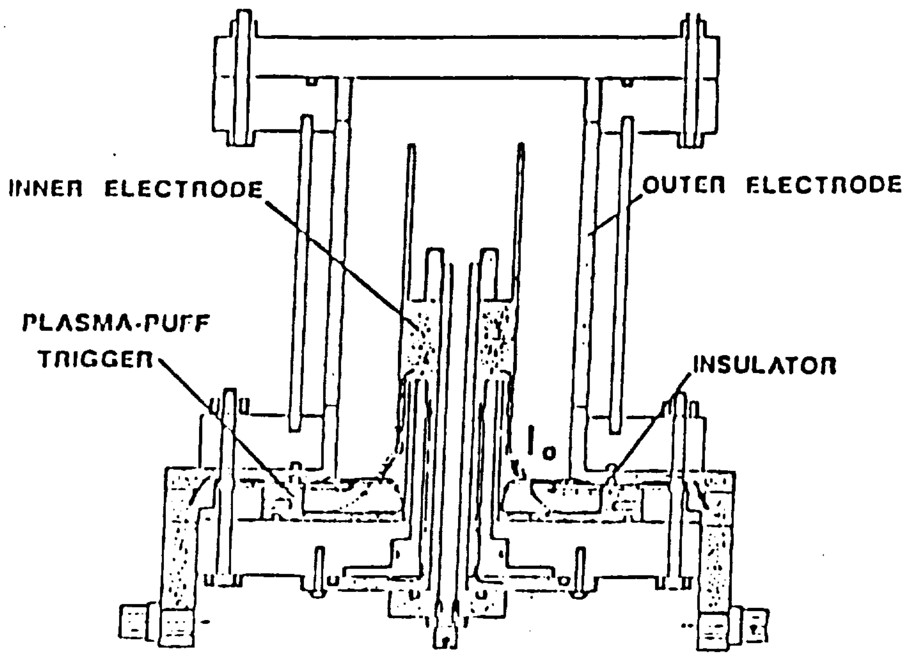

Figure 2b. Inverse-pinch combined with the hypocycloidal-pinch plasma-puff device.

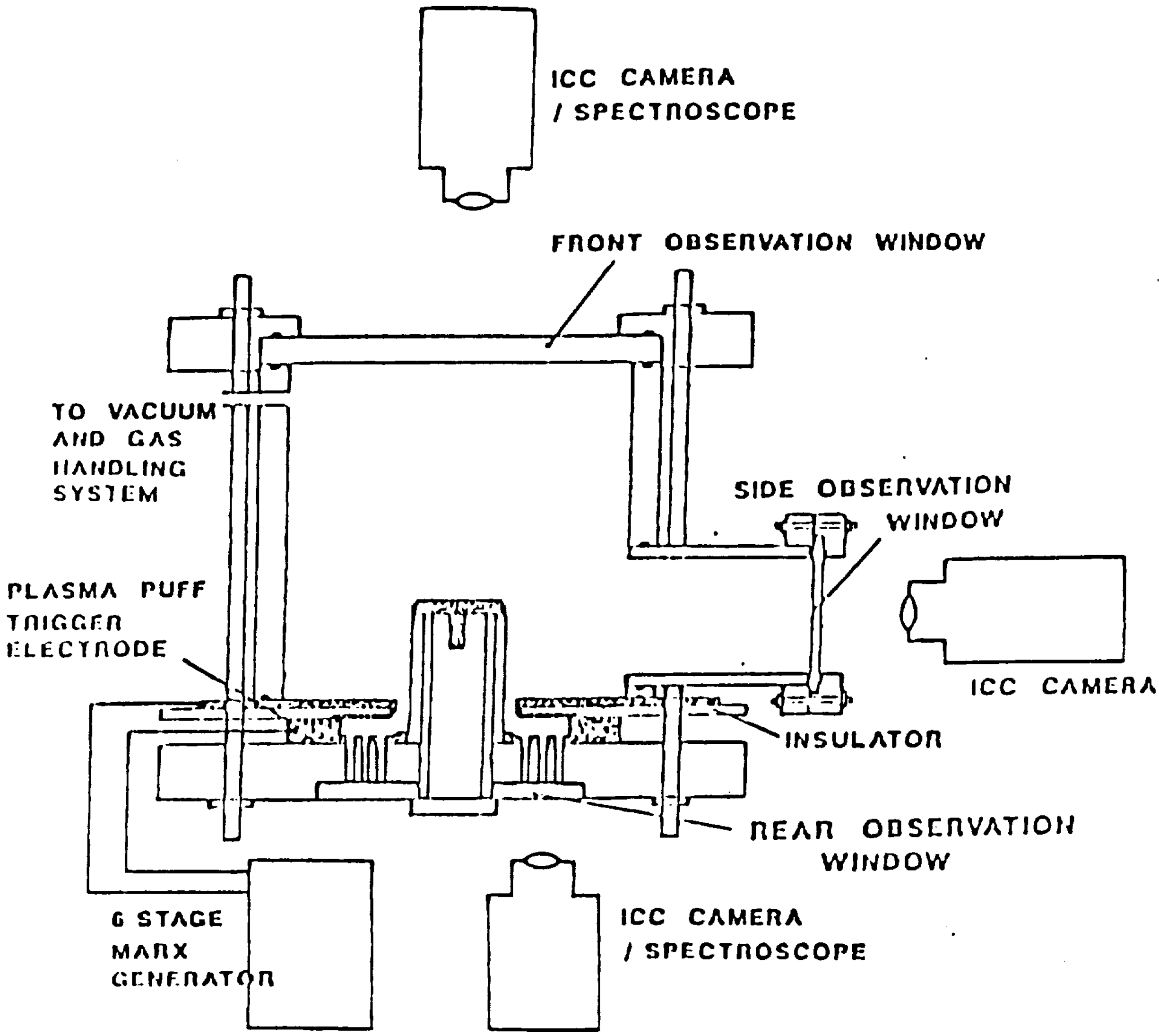

Figure 4. Schematic diagram for the spectroscopic and plasma dynamic measurements of the hypocycloidal pinch plasma-puff produced plasma.

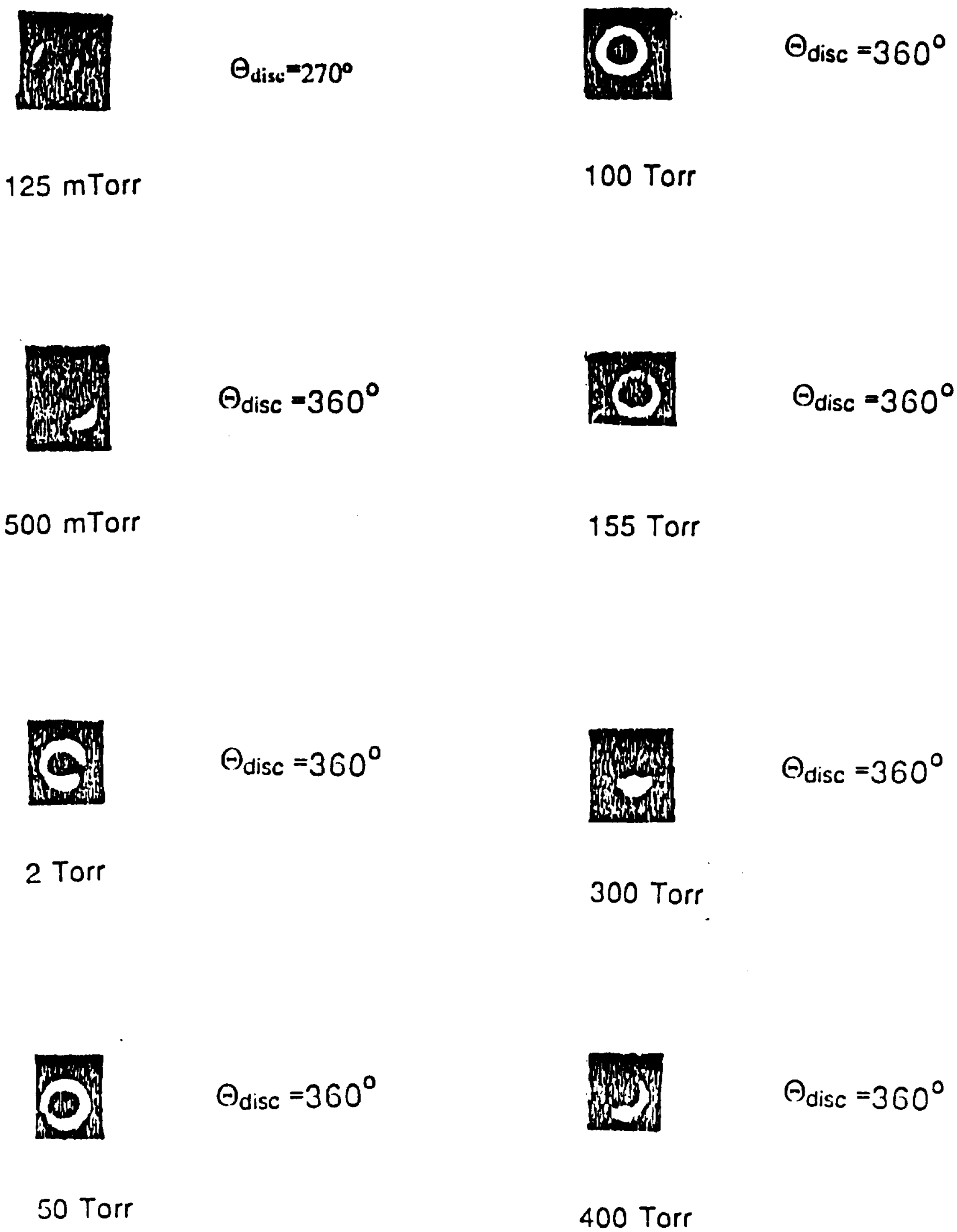

Figure 5. ICC Focussing mode picture for the surface breakdown of hypocycloidal pinch plasma-puff at several N_2 gas pressures for a charging voltage of 15 kV to the Marx generator.

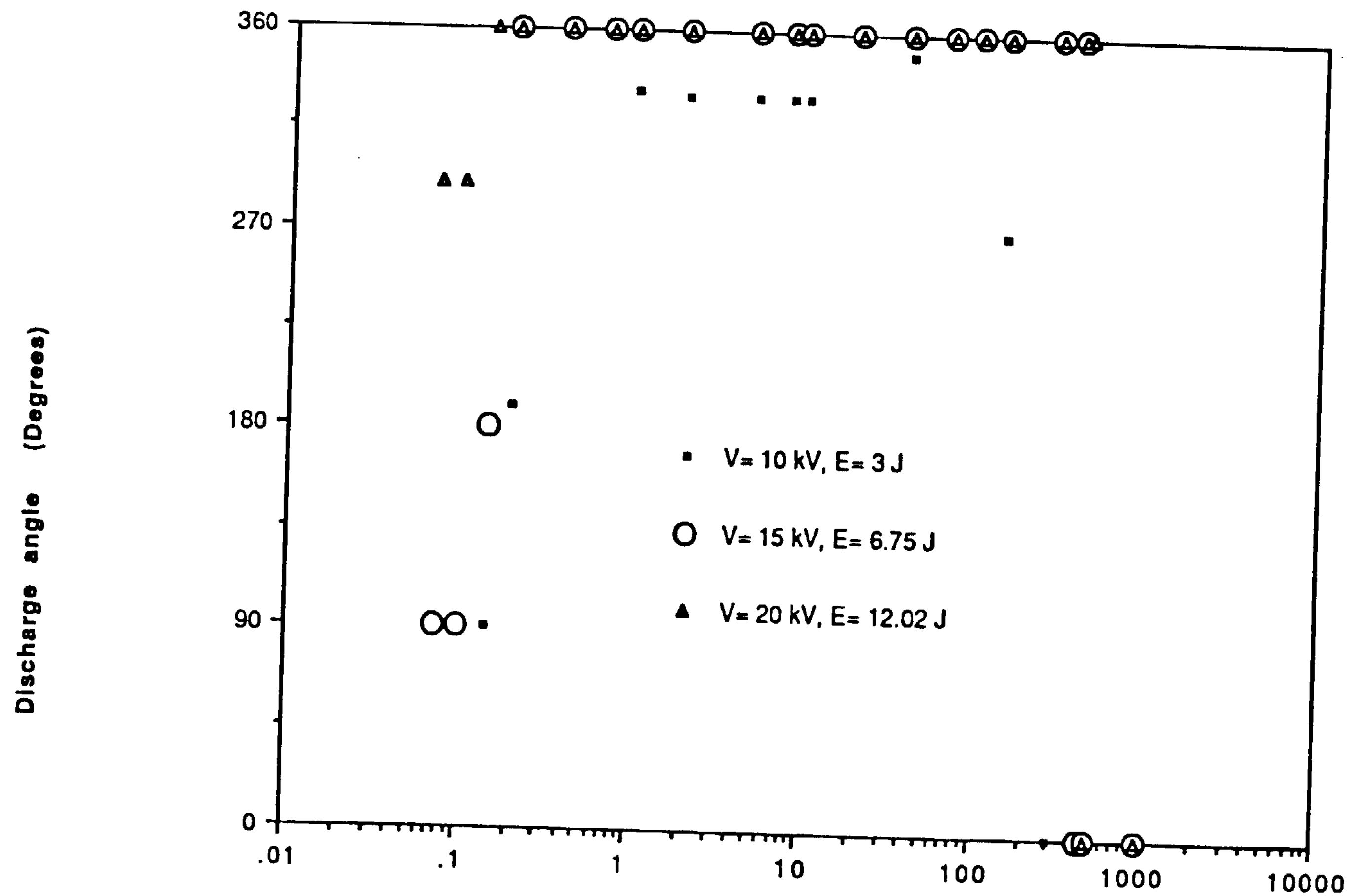

Figure 6a. Discharge angle (θ_{disc}) versus nitogen gas pressure for hypocycloidal pinch plasma-puff trigger. Solid squares, circles and triangles correspond to the charging voltages of 10 kV, 15 kV and 20 kV, respectively, to the Marx generator.

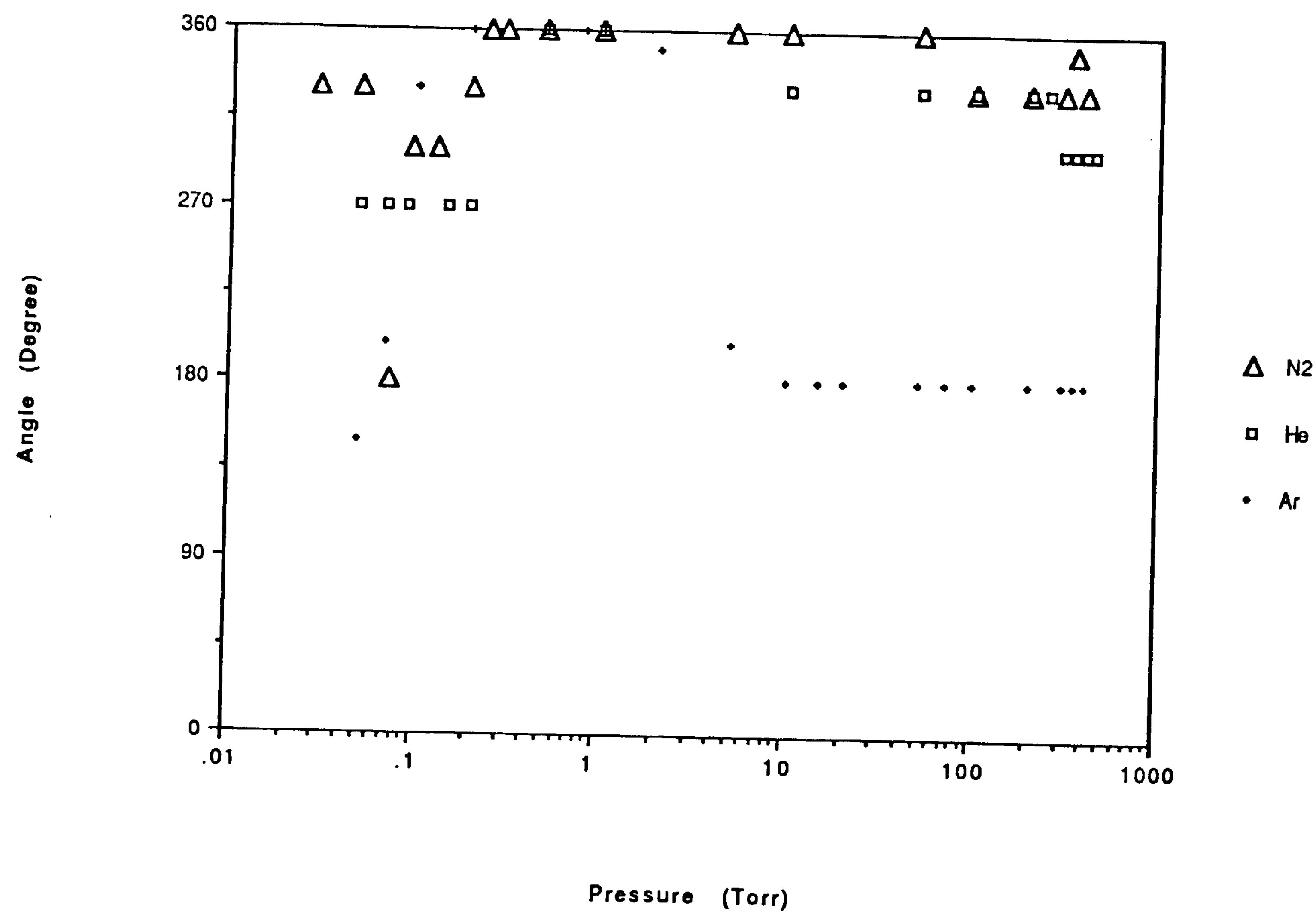

Figure 6b. Angle of plasma emission versus gas pressure of Ar, He and N_2 for hypocycloidal pinch plasma-puff trigger under the charging voltage of 15 kV to the Marx generator. Triangles, squares and crosses correspond to N_2, He and Ar, respectively.

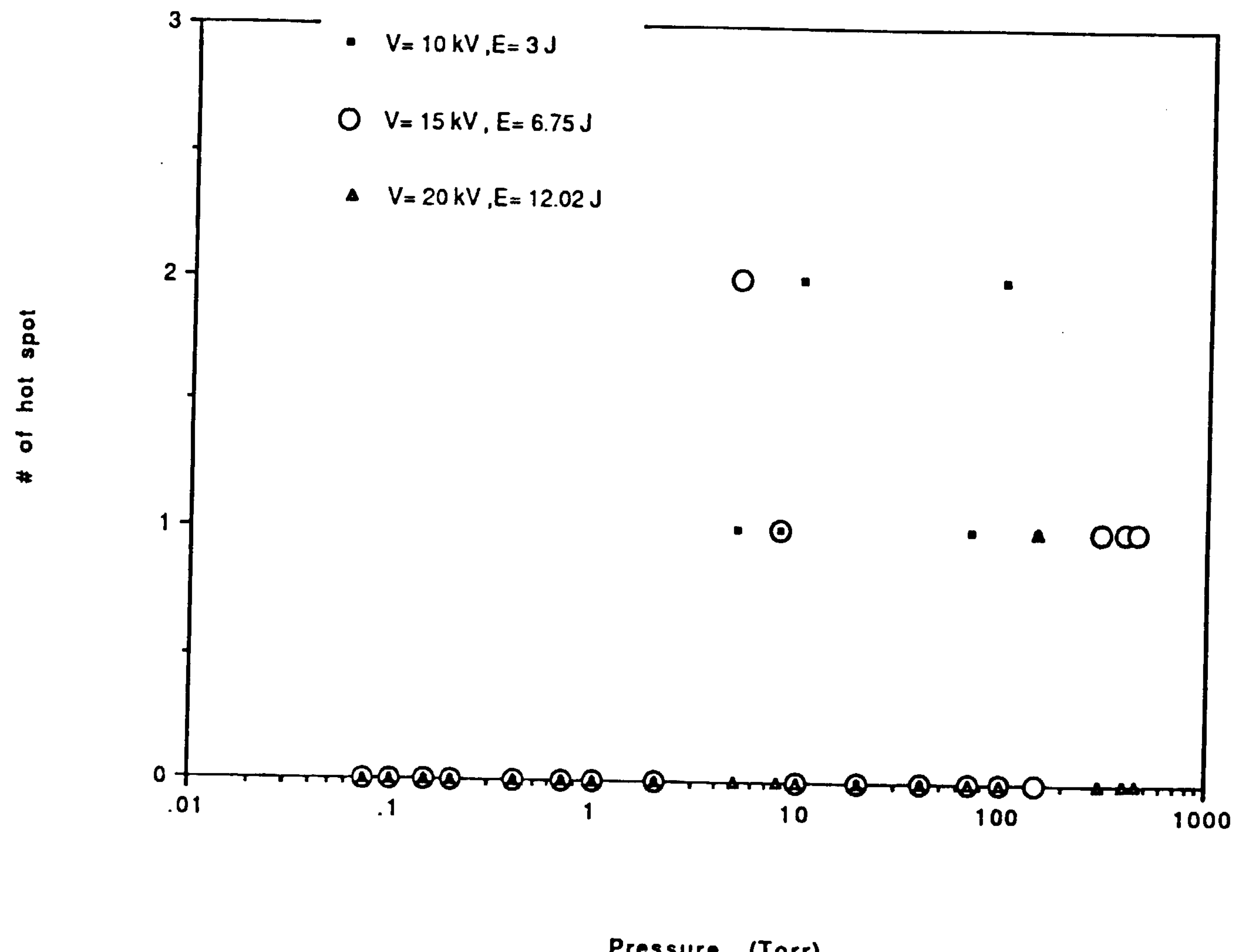

Figure 7. Number of hot spots versus nitrogen gas pressure for hypocycloidal pinch plasma-puff trigger. The symbols used here are identical with those of Fig. 6a.

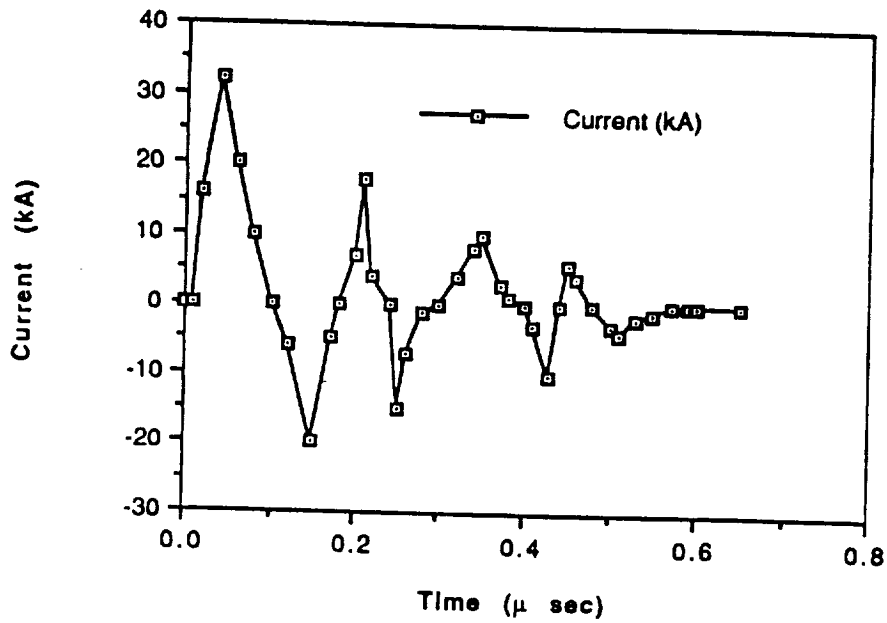

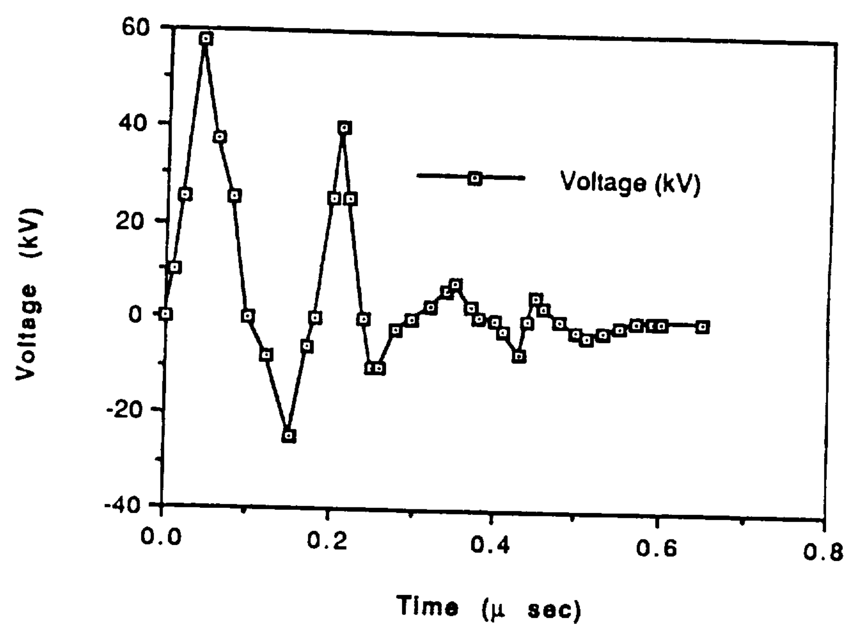

Figure 8. Triggering current (upper) and voltage (lower) waveform versus time for hypocycloidal pinch plasma- puff. These data were obtained with a gas pressure of 4 Torr and a charging voltage of 10 kV to the Marx generator.

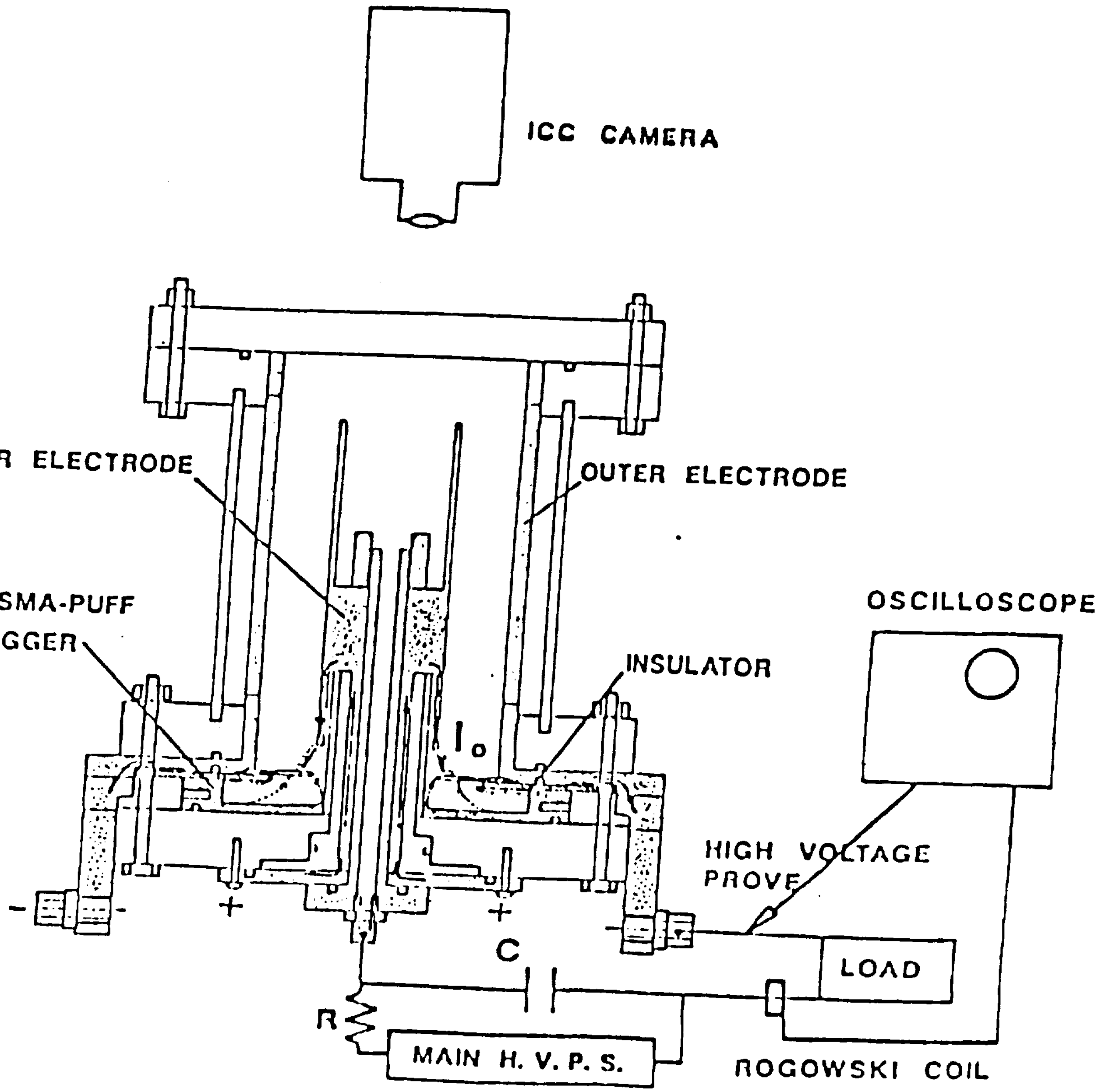

Figure 9. Schematic diagram of the diagnostic equipment of the inverse pinch switch with the hypocycloidal pinch plasma-puff trigger.

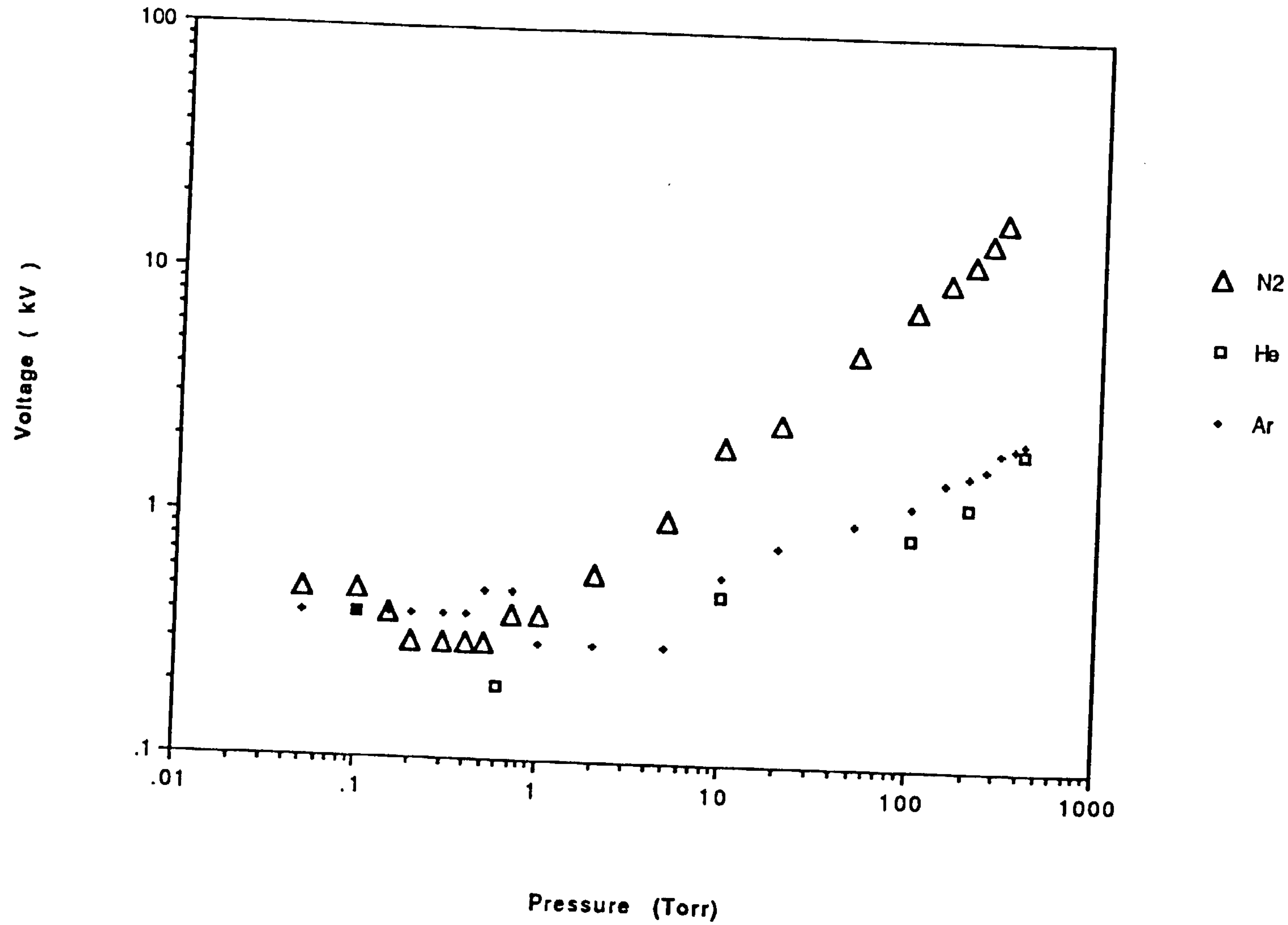

Figure 10. Hold-off voltages of the inverse pinch switch versus gas pressures of Ar, He and N_2. Crosses, squares and triangles correspond to the gases of Ar, He and N_2, respectively.

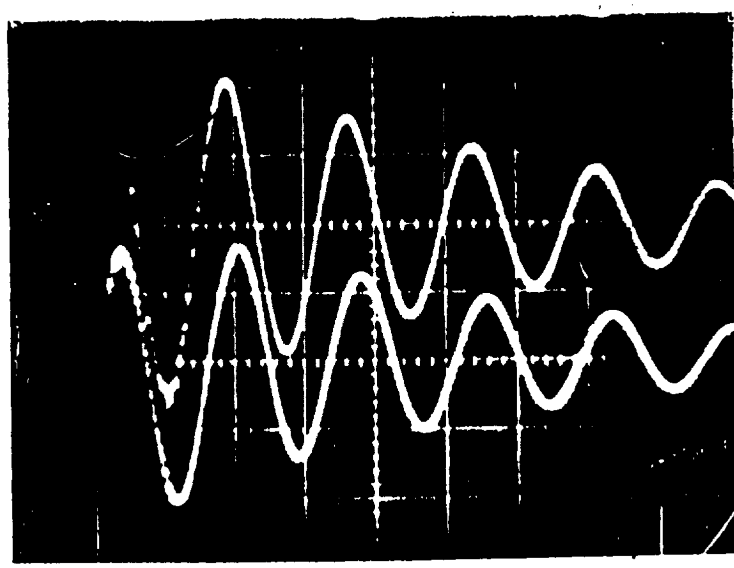

Figure 11. Voltage (upper) and current (lower) waveforms of inversepinch switch versus time. These data were obtained for a N_2 gas of 300 Torr under charging voltage of 13.5 kV to inner electrode of inverse pinch switch.

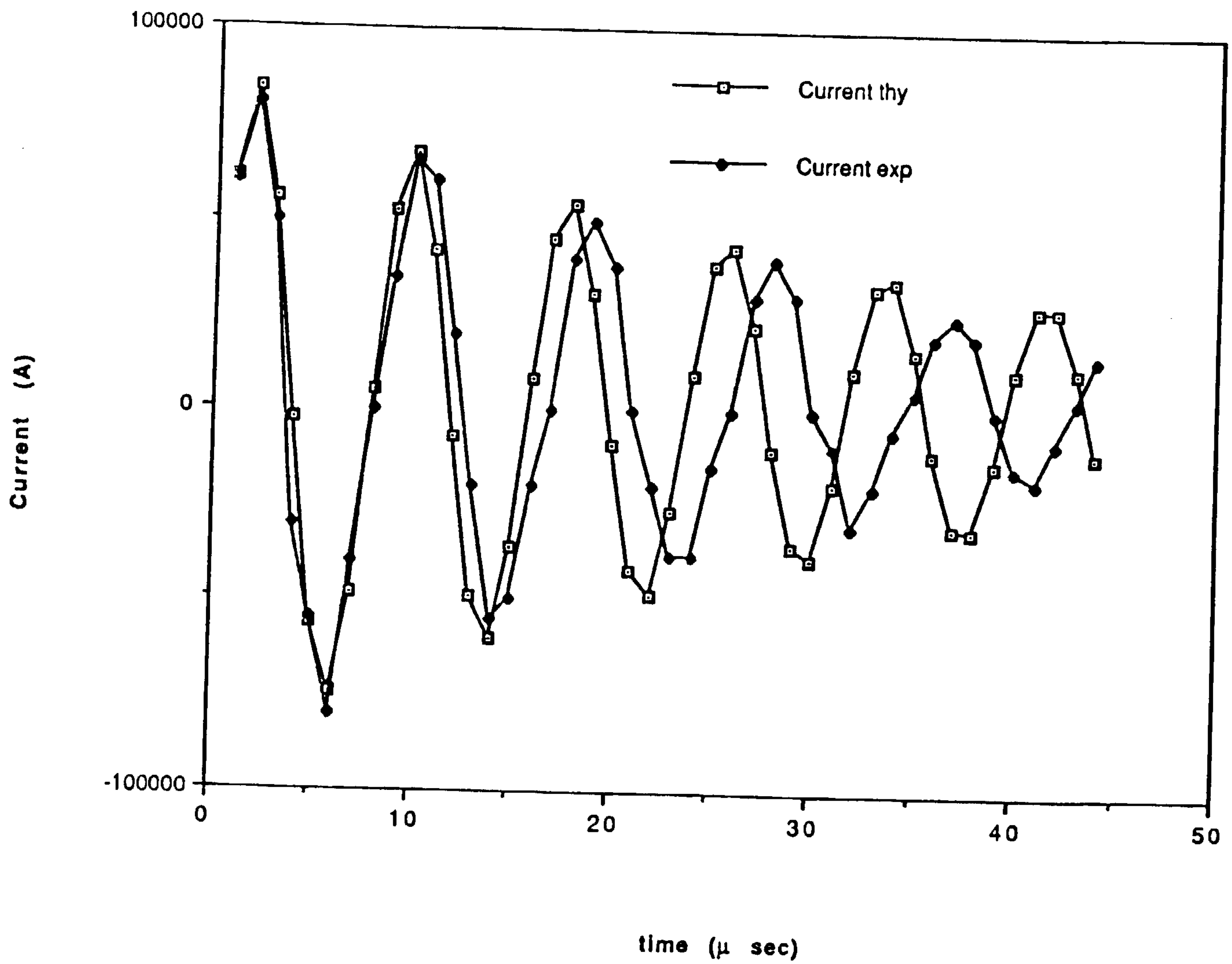

Figure 12. Measured and calculated current waveforms of the inverse pinch switch versus time. Solid squares and squares correspond to the measured and calculated values, respectively. These data were obtained under charging voltage of 13.5 kV to inner electrode of inverse pinch switch.

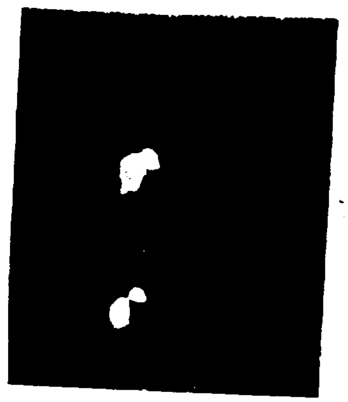

Figure 13. Frame mode photograph of the breakdown of the inverse pinch switch with the hypocycloidal pinch plasma-puff trigger taken by the image converter camera with the first and second delay times of 1.2 us and 0.5 us,respectively. The main charging voltage is kept at 9 kV and the N_2 gas pressure is maintained at 150 Torr.

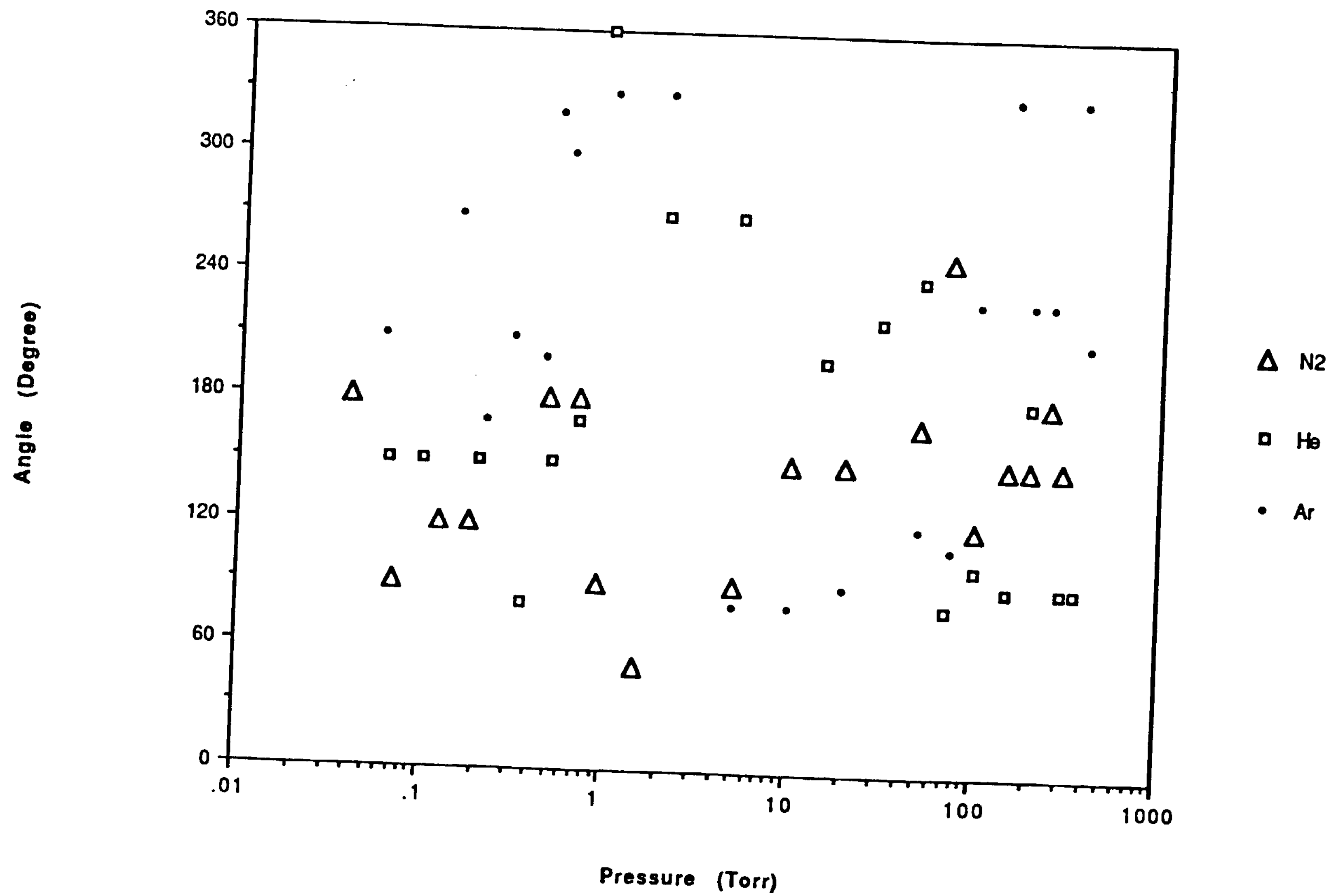

Figure 14. Main discharging angles of inverse pinch switch with hypocycloidal pinch plasma-puff trigger versus pressure for gases of Ar, He and N_2. Triangles, squares and dots correspond to the N_2, He and Ar, respectively.

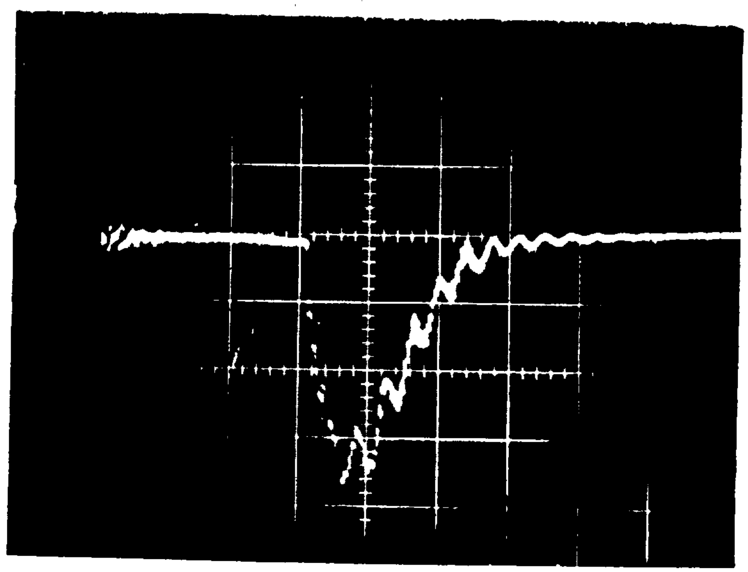

5 μs/div

Time

Figure 15. Triggering voltage waveform of plasma-focus driven plasma-puff versus time. This can be obtained under N_2 gas pressure of 40 mTorr.

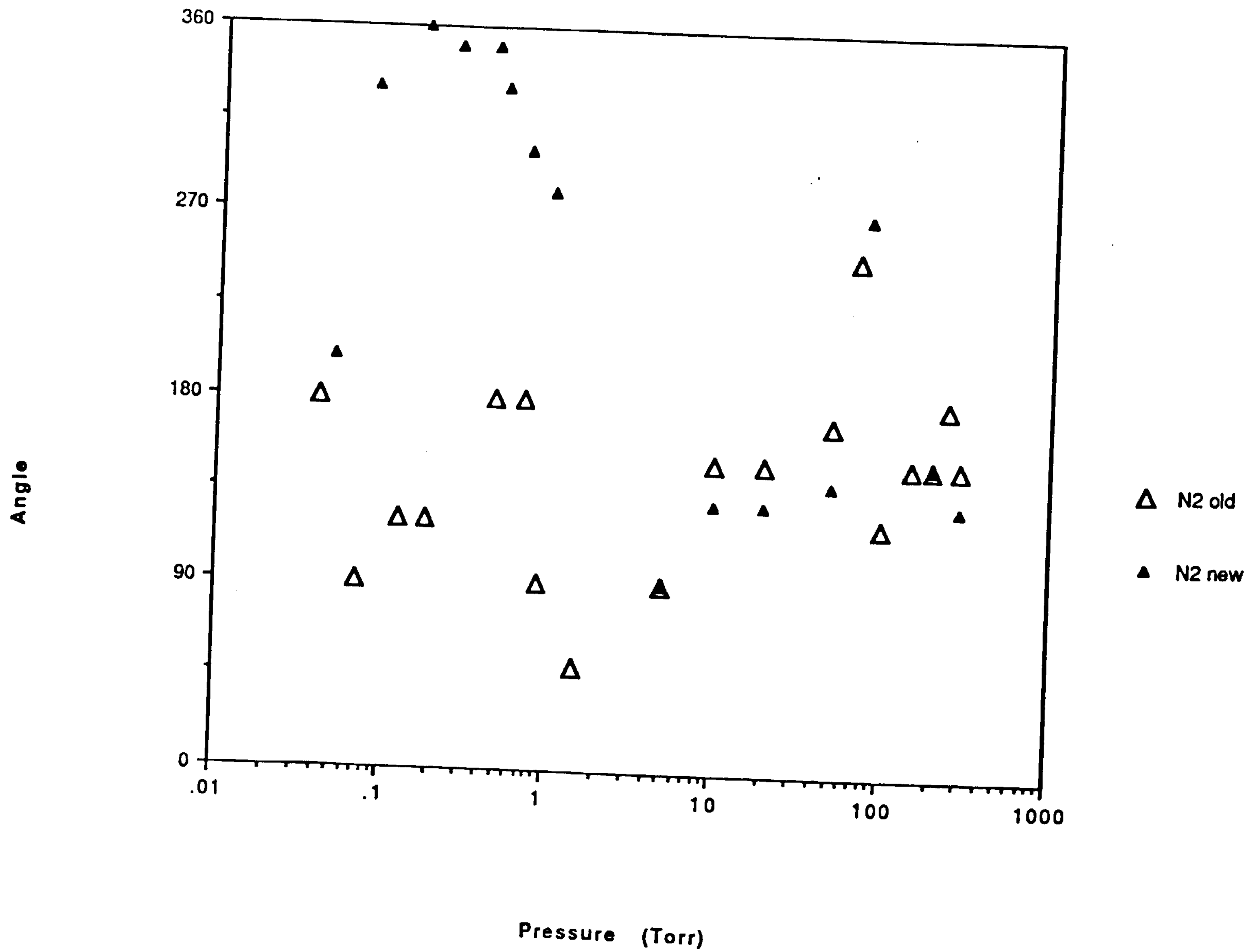

Figure 16. Main discharging angles of inverse pinch switch versus N_2 gas pressures with plasma-focus driven plasma-puff trigger and hypocycloidal pinch plasma-puff trigger. Solid triangles and triangles correspond to the plasm-focus driven plasma-puff trigger and hypocycloidal pinch plasma-puff trigger, respectively.

Figure 17. Focussing mode photograph of the azimuthally uniform breakdown of the inverse pinch switch with the plasma-focus driven plasma-puff trigger taken by the image converter camera. The first and second delay times are set to be 1.2 us and 0.5 us, respectively. The N_2 gas pressure is kept at 80 mTorr.

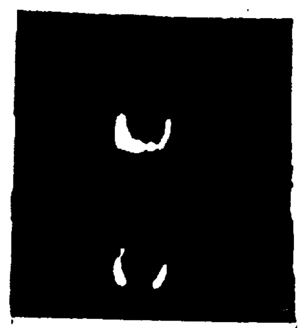

Figure 18. Frame mode photograph of the uniform breakdown of the inverse-pinch switch with the plasma-focus driven plasma-puff trigger taken by the image converter camara with the first and second delay times of 1.2 μs and .5 μs, respectively at a gas pressure of 800 mTorr.